EPRG-PRCI-APGA
23rd Joint Technical Meeting
Edinburgh, Scotland
6–10 June 2022

PAPER TITLE: ASSESSING THE COMPATIBILITY OF CURRENT PLASTIC AND ELASTOMERIC MATERIALS USED WITHIN THE AUSTRALIAN GAS PIPELINE NETWORK WITH HYDROGEN-CONTAINING FUEL

PAPER NUMBER: 29

Nolene Byrne
Institute for Frontier Materials, Deakin University, Waurn Ponds, Victoria, Australia.

Sebastian Manjarres Espinosa
Institute for Frontier Materials, Deakin University, Waurn Ponds, Victoria, Australia

Sadegh Ghanei
Institute for Frontier Materials, Deakin University, Waurn Ponds, Victoria, Australia

Nicholas Kastelein*
GPA Engineering, Adelaide, South Australia

* presenting author

ABSTRACT

The energy sector worldwide is seeking to decarbonize and this has led to rapid change and development in the sector. In Australia, the gas sector has a vision to be near zero carbon by 2050. The most promising route towards achieving this target is the replacement of methane with hydrogen. Hydrogen is currently being intensely investigated as a green fuel source. Many aspects of converting to a hydrogen economy still require research, these include the suitability of current gas transporting infrastructure to transport hydrogen. To address this question our research team is investigating the interactions of hydrogen with i) the plastic pipe materials namely various resin types of polyethylene and ii) elastomer materials found in the o rings, diaphragms and gaskets within a typical distribution network. This conference paper will detail the findings for our elastomer studies as well as a comment on how hydrogen influences the slow crack growth resistance of PE pipes.

DISCLAIMER

1. INTRODUCTION

As Australia, and many other countries worldwide, seeks to lower their carbon footprint, the utilization of "carbon zero" hydrogen as a fuel source has attracted considerable interest. The Australian gas sector has a vision to be near zero carbon by 2050, and the most promising route towards achieving this from an economic and technical perspective is replacing fossil fuels with hydrogen. Many aspects of converting to a hydrogen economy require further research [1-5]. In this research paper the influence of hydrogen on the properties of key elastomers as well as on the failure of polyethylene pipes and in particular the slow crack growth behaviour is discussed

1.1. Elastomers and Hydrogen

A large number of different materials exist within the network. This is particularly true for the elastomer parts of the network. Elastomers are a key material class used within the gas network, across the transmission, distribution and end user network. E, elastomers are used as o-ring, gaskets, diaphragm as other sealing components and within some joining approaches [6-8]. Since elastomers are found in many places within the gas network the type of elastomer utilized can also vary greatly often dictated by the pressure used [6]. Perhaps one of the most common elastomer types is butadiene rubber, either styrene-butadiene or acrylonitrile-butadiene rubber (NBR). NBR is a synthetic unsaturated statistical copolymer of acrylonitrile and butadiene [9]. NBR has good oil and chemical resistance and reasonable operating temperature range. Besides the gas sector NBR is used in the automotive and petroleum industries for oil and engine fuel transport equipment, for machinery pumps and in disposable non-latex gloves. The properties of NBR are influenced by the amount of acrylonitrile content, the plasticizer and the filler amount and type. Carbon black is the most common filler type used in commercial rubbers, including most NBR types [10, 11].

While NBR has good compatibility with methane its performance with hydrogen is relatively unknown. Limited literature is available on the compatibility of elastomers with hydrogen. The majority of hydrogen/elastomer studies have been conducted at high pressure more representative of fuel cell and refuelling station applications, however, the literature indicates that NBR shows material property changes with hydrogen exposure [14,15]. The reported property changes are greatly influenced by the filler type, filler amount and plasticizer choice or auxiliary packages. It is common that manufactures and suppliers of NBR often use different plasticers and auxiliary packages covered by IP and unknown to the user. Here we tested the response of two NBR70 elastomers purchased from two different suppliers. Included in the study is HNBR (Hydrogenated Nitrile Butadiene Rubber) which is considered to be a technical elastomer often found in higher pressure more extreme applications.

1.2. Failure of Polyethylene

The service life of PE pipes is often considered to be linked to the Slow Crack Growth (SCG) resistance and subsequently failure resistance of the PE resin. Currently, no available literature exists investigating the impact hydrogen exposure has on the SCG performance of PE pipes.

Three distinct modes that correspond to the circumferential tensile stress in the pipe wall are associated with PE pipe failure [16,17] The first failure mode is called ductile failure which is associated with the creep expansion of the PE pipe that occurs at high stresses as a result of localised yielding and bulging out at the stress concentration sites [18,19]. The second and most commonly experienced mode of failure reported for PE pipes in the field is typically termed quasi-brittle associated with SCG through the pipe wall. This failure mode initiates from a stress-raising defect in the pipe when the circumferential tensile stress is lower than the stress level which is required for ductile failure [20,21]and often lower than the yield strength of the material. The last failure mode; brittle failure, occurs after a long period of service time when the circumferential tensile stress is further reduced [20,22]. In this mode, the applied stress has little impact on the service life of the pipe and the failure initiates due to ageing and polymer degradation. Since the quasi-brittle failure is the most common failure mode for in-service PE

pipes, the SCG resistance determines the service life of the PE pipe [16,24]. Therefore, the study of SCG performance plays an important role in indicating the service life of the PE pipe when transporting hydrogen and is the topic discussed in this conference paper.

In literature there are numerous approaches to measure the SCG performance of PE resins; all involve an accelerating agent which may be elevated temperature and/or a pre-existing notch in the test samples. Evaluating the SCG behaviour using elevated temperature may face some issues such as the poor or even inverse relationship between the time to failure at elevated and room temperatures [25-26], and presenting macroscopic ductile fracture components which do not necessarily exist at service temperature. Another option to shorten the test time and rank the SCG resistance is to introduce a notch in the samples [24] using methods like Cracked Round Bar (CRB) test [27], Full Notch Creep Test (FNCT)[28], Pennsylvania Edge Notch Test (PENT)[29]. Among these various techniques, the CRB test has been successfully used in several studies of the SCG behaviour of PE resins including modern resins with excellent SCG resistance. Using cyclic loading and a notch accelerates the test while allowing the temperature to be at room temperature and thus SCG ranking is more representative of field service like failure. Despite providing valuable information regarding the service life of various PE pipes, some limitations are associated with the CRB method. The standardised CRB test requires samples with a diameter of more than 10 mm [27] which cannot be met by many of the available PE pipes in the natural gas distribution network [16] meaning that test samples cannot be sectioned directly from the pipe wall and moulding is required which may result in a change of properties or slight degradation during the moulding process, particularly for vintage in-service pipes. To overcome this limitation, the Cyclic PENT (CPENT) geometry was developed by this team, which investigates notched rectangular samples [16]. The CPENT is able to study samples that are directly sectioned from the PE pipe wall.

2. METHODS

2.1. Elastomers

2.1.1. Hydrogen gas exposure protocol

Samples were exposed to hydrogen gas at room temperature (~25°C) at varying pressures and times in a 0.6 litre Parr 4760 series stainless steel pressure vessel equipped with a Pressure display module. The system was purged in cycles 1 barg – 40 barg – 1 barg with a non-flammable gas to bring the concentration of oxygen present in the vessel below 0.10% before admitting hydrogen. Subsequently, the system was purged with high purity hydrogen gas following the same cycle protocol until a concentration of ~ 99.95% hydrogen was achieved

2.1.2. FTIR: Fourier-Transform Infrared Spectroscopy

The FTIR spectra of the samples before and after exposure to hydrogen were taken using a Bruker LUMOS FTIR microscope in the frequency range of 600 cm-1 to 4,000 cm-1 at a scan resolution of 4 cm-1. A background and sample scan time of 64 scans was used for all samples.

2.1.3. Dynamic Mechanical Analysis

A TA Q800 DMA analyser in dual-cantilever mode was used to investigate the dynamic mechanical properties of the samples before and after exposure to hydrogen. Samples were sectioned from sheets in a rectangular shape with dimensions 60mm L x 12mm W x thickness of sheet. The samples were subjected to a controlled-strain force with a varying frequency between 0.1 to 20 Hz at an amplitude of 15 µm at 20°C, 35°C and 75° isothermal conditions, and the storage modulus, loss modulus and tan delta calculated.

2.1.4. Compression Set and recovery rate

Compression set is often a property of interest when studying elastomeric materials, especially those used to create seals. It measures the ability of a rubber to return to its original thickness after a prolonged compressive stress at a specific deflection and temperature. Samples were compressed to ~ 25% of their original thickness following the ASTM D395 – Test Method B and exposed to hydrogen gas at room temperature at varying pressures and times. The exposure to hydrogen occurred with the samples in the compression state inside the pressure vessel, and subsequently the samples were removed and measurements taken ex-situ. The compression set values were calculated using equation 1. at given time intervals; where t_0 is the original thickness, t_1 is the final thickness and t_n corresponds to the spacer thickness. A % recovery rate is plotted comparing the change in height of the sample compared to original height.

$$CB\ (\%) = \left(\frac{t_0 - t_1}{t_0 - t_n}\right) * 100 \qquad (1)$$

2.1.5. Compression Set and recovery rate

The CPENT of exposed and unexposed samples were conducted at various stress concentration factors, ΔK, which can be calculated as follows [6, 23]:

$$\Delta K = \Delta\sigma \times \sqrt{\pi \times a} \times \left[1.12 - 0.23\left(\frac{a}{b}\right) + 10.56\left(\frac{a}{b}\right)^2 - 21.74\left(\frac{a}{b}\right)^3 + 30.42\left(\frac{a}{b}\right)^4\right] \qquad \text{Eq. 1}$$

where Δσ, *a* and b are the difference between the minimum and maximum applied stresses, the initial depth of the notch, and the sample thickness, respectively. For PE63 and PE80B pipes exposed to hydrogen at 80Bar for various time intervals up to 90 days.

2.1.6. Cyclic Pent

The CPENT of exposed and unexposed samples were conducted at various stress concentration factors, ΔK, which can be calculated as follows

$$\Delta K = \Delta\sigma \times \sqrt{\pi \times a} \times \left[1.12 - 0.23\left(\frac{a}{b}\right) + 10.56\left(\frac{a}{b}\right)^2 - 21.74\left(\frac{a}{b}\right)^3 + 30.42\left(\frac{a}{b}\right)^4\right] \qquad \text{Eq. 2}$$

where Δσ, *a* and b are the difference between the minimum and maximum applied stresses, the initial depth of the notch, and the sample thickness, respectively. For PE63 and PE80B pipes exposed to hydrogen at 80Bar for various time intervals up to 90 days.

3. RESULTS AND DISCUSSIONS

3.1.1. Elastomers and Hydrogen

Table 1 lists all the elastomers used in this study and some of their main properties.

Table 1. Materials part of this study.

Sample label	Colour	Shore A Hardness	Specific Gravity	Tensile Strength	Elongation at Break	Supplier*
NBR70_S1	Black	65 ± 5	1.20	15.0 MPa	400%	Supplier 1
NBR70_S2	Black	65 ± 5	1.20	15.0 MPa	400 %	Supplier 2
HNBR	Light brown	70 ± 5	0.96	TBC	TBC	Supplier 3

*Supplier 1 is SealTeam www.sealteam.com.au; Supplier 2 is Complete Rubber www.completerubber.com.au; and Supplier 3 is Arlanxeo www.arlanxeo.com.

Figure 1a-c shows the storage modulus as a function of frequency measured at 20°C, 35°C and 75°C respectively for the unexposed NBR and H_2 gas exposed NBR samples whereby exposure was for 7 days at 80 bar for NBR70 supplier 1 and NBR70 supplier 2. From Figure 1 it can be seen that for the non exposed samples (solid lines where black is NBR70 supplier 1, red is NBR70 supplier 2) the storage modulus is reasonably similar for the two NBR70 samples irrespective of supplier. This is an expected trend as the temperature increase the storage modulus of each unexposed NBR sample decreases, again this is an expected trend as temperature increases the mobility of the polymer chains resulting in a more rubbery material with a lower stiffness.

For the samples which have been exposed to H_2 gas the trend is dictated by the supplier. For NBR70 supplier 1, black dotted line, the sample which was exposed to hydrogen shows a significant increase, 140%, in storage modulus especially measured at 20°C Figure 1a and 35°C Figure 1b, indicating the elastomer has become stiffer. The impact of hydrogen is lessened at 75 °C for NBR70 supplier 1. This suggests that the hydrogen compatibility of NBR70 supplier 1 improves with temperature and is likely due to the overall increase in polymer chain mobility and thus any hydrogen which maybe trapped in the sample is not as detrimental as the temperature increases.

The influence of H_2 gas exposure is however opposite for NBR70 supplier 2 (red dotted line is exposed), here the storage modulus is reduced slightly showing an approximate 12% reduction at 10Hz at each temperature measured. Thus, for the NBR70 from supplier 2 the exposure to H_2 gas for 7 days at 80 bar have little influence on the storage modulus and no temperature effect was measured suggesting that this elastomer has excellent hydrogen compatibility.

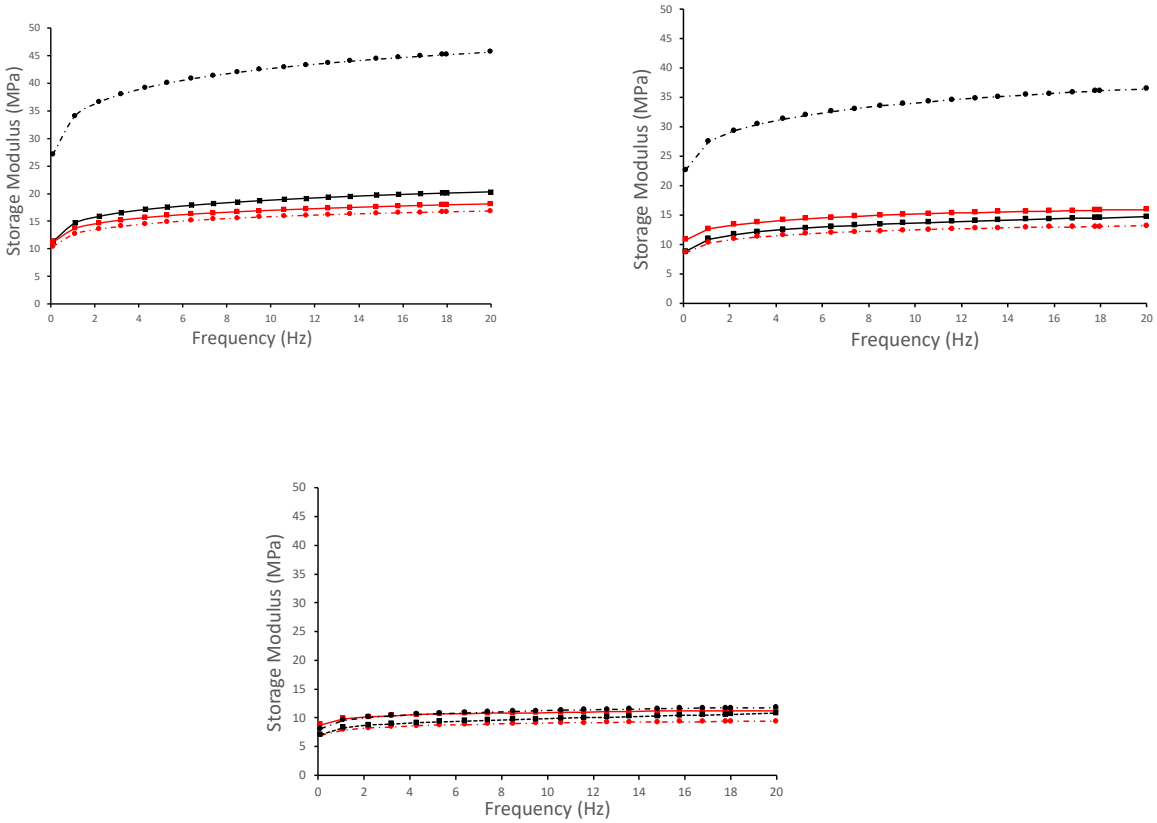

Figure 1: Storage modulus (MPa) as a function of frequency for a) 20°C b) 35°C and c) 75°C where NBR70supplier 1 non exposed (black solid line) exposed (black dotted line) NBR70supplier 2 non exposed (red solid line) exposed (red dotted line)

The increase in stiffness as a function of hydrogen exposure for NBR70 supplier 1, can be recovered if the elastomer is removed from the H_2 gas for a sufficient amount of time. Figure 2 shows the storage modulus as a function of frequency measured at 35°C for the unexposed (black curve), exposed 7 days at 80Bar measured 24 hours after removed from the H_2 gas (red curve), and the exposed 7days at 80Bar and measured 2 weeks after removal from the H_2 gas (green curve). It can be seen that an almost full recovery is achieved suggesting no permanent changes has occurred under these exposure conditions. The FTIR supports no permanent change with H_2 gas exposure under these conditions as no change in the spectra has been detected

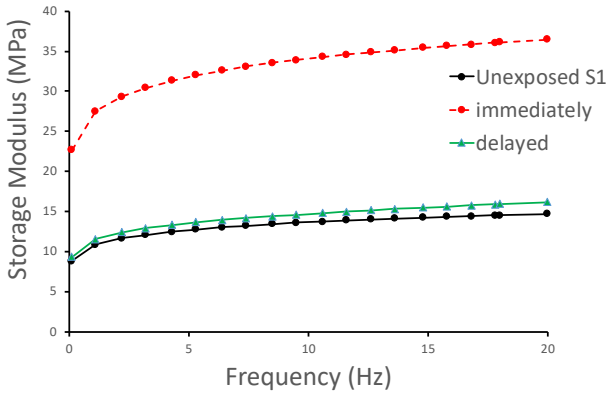

Figure 2: Storage modules as a function of frequency for NBR70 supplier 1 measured at different time intervals after H_2 exposure.

Figure 3 shows the recovery rate for NBR70 supplier 1 as a function of pressure for a fixed 7day exposure, here the sample is compressed to 25%. The % recovery is measured as the change in height in relation to the original non compressed sample at different time intervals. It can be seen that the % recovered is influenced by the pressure used, where samples exposed to 80bar showed the slowest recovery rate, while the sample exposed to 5bar had an improved recovery rate, regardless of pressure the sample never returns to the same %recovered as the unexposed sample suggesting that hydrogen has modified the elastomers response and ability to recovery after compression.

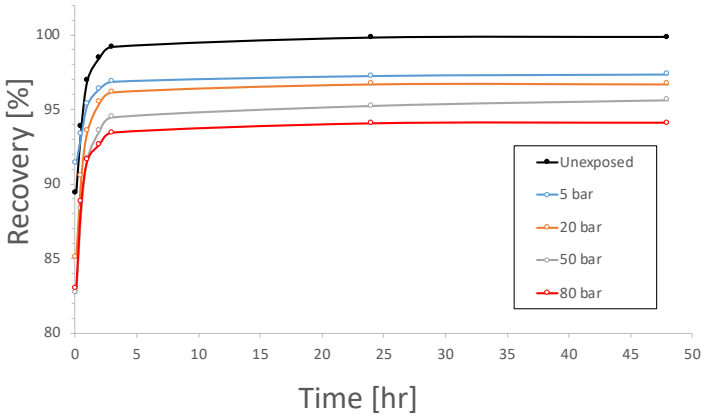

Figure 3: % Recovery as a function of pressure for NBR70 supplier 1

In comparison the trend for NBR70 supplier 2 is in contrast to NBR70 supplier 1, Figure 4 shows the % recovery rate for NBR70 supplier 2 exposed to H_2 gas at 80 bar for 7days. The exposed sample shows an improved recovery rate which maybe linked to improved flexibility and a pseudo plasticization effect.

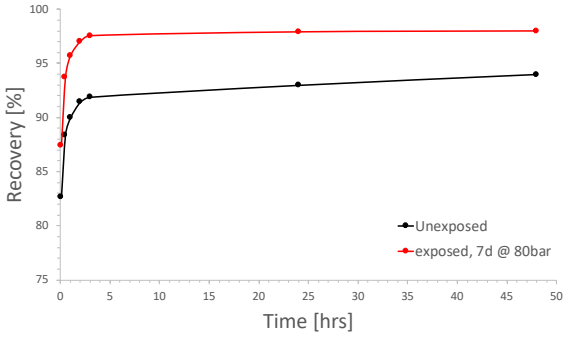

Figure 4: % recovery rate as a function of time for NBR70 supplier 2 exposed to H_2 for 7 days

NBR is a common non technical elastomer found in the oil and gas industry. For higher pressures often more advanced technical grade elastomers with improved mechanical strength and chemical resistance are utilized, with HNBR commonly used as a technical elastomer within the gas industry. Figure 5 shows the storage modulus as a function of frequency for HNBR at 20°C (black), 35°C (blue) and 75°C (red) for non exposed (solid line) and exposed (dotted line). As expected, the storage modulus decreases with temperature for both exposed and unexposed, however as can be seen the storage modulus also decreases for samples exposed to H_2 gas when compared to the non exposed sample. This trend is opposite to NBR70 supplier 1, furthermore even at 75°C a difference between exposed and unexposed is measured. Again this is different to the non technical NBR variants and likely due to the higher cross linked density of HNBR. The storage modulus is reduced by more than half across all temperatures when exposed to hydrogen.

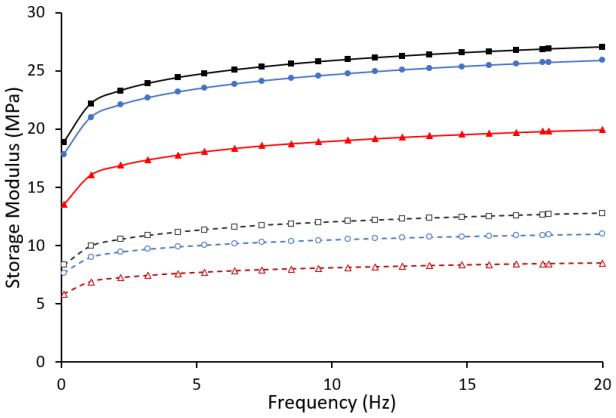

Figure 5: Storage modulus as a function of frequency for HNBR unexposed (solid lines) and exposed (dotted lines) at 20°C (black), 30°C (blue) and 75°C (red).

3.1.2. Failure of Polyethylene

Figure 6 compares the time to failure for the two vintage PE pipe resin types at different stress concentration factors for non-exposed samples. Testing at the same stress concentration factor, PE80 pipe shows a higher fatigue resistance than PE63 which is represented by the longer time to failure, PE80 is known to have a higher SCG resistance when compared to PE63, due largely to the difference in molecular weight distribution and crystallinity.

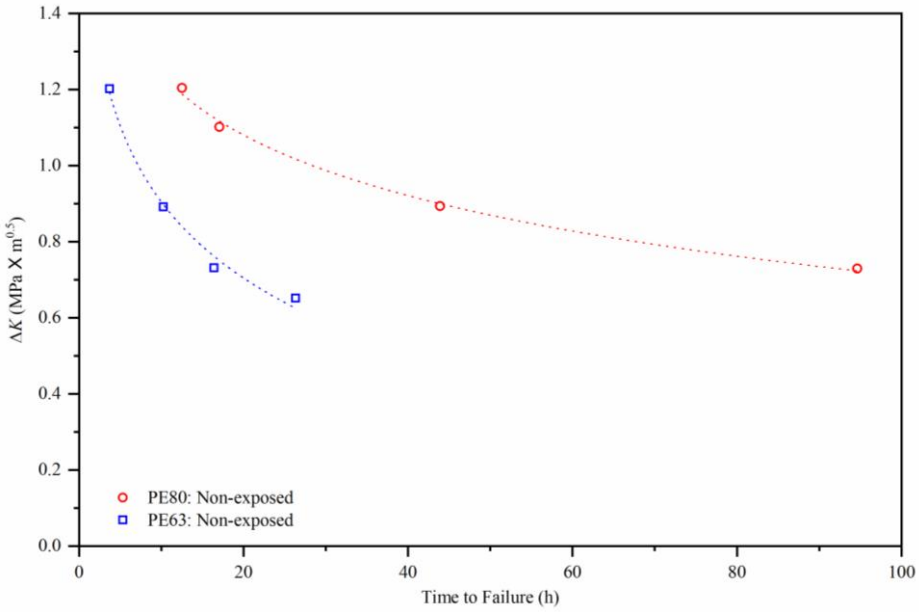

Figure 6. Time to failure as a function of ΔK for PE63 and PE80 pipe samples.

Identifying stable crack growth Figure 7 *a* shows the fracture surface of the PE80 sample with no exposure to hydrogen in which the CPENT was carried out at ΔK=1.20 MPa[m^0.5]. Below the notch area, the fatigue striation marks can be observed even at a low magnification, which are followed by a distinctive ductile failure region (Figure -*a*). These fatigue striations are true crack arrest markings on the fracture surface of polymers [24]. As can be observed in Figure -b, for each striation, the damage accumulation continues in the craze zone until reaching a point where the next cycle of loading results in jumping the crack tip to the craze boundary and forms a striation; then, this process repeats, and the formation of the next striation starts.

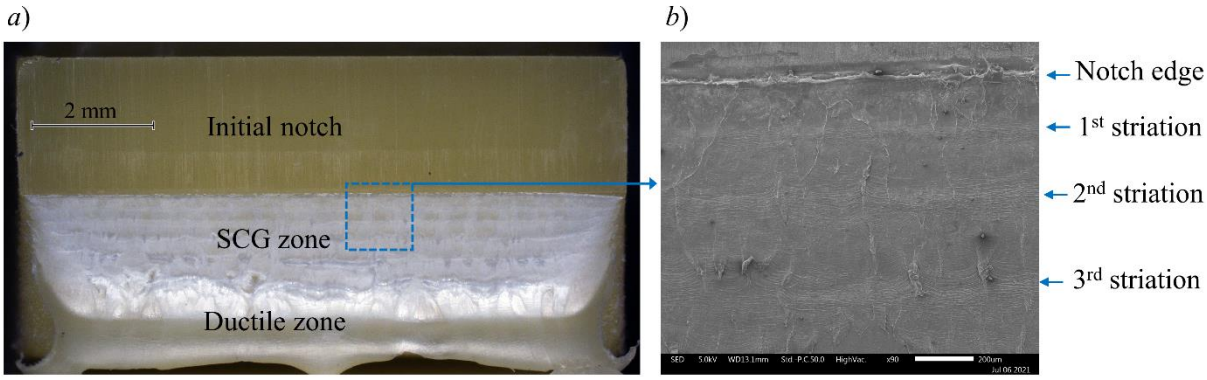

Figure 7. The fracture surface of PE80 sample with no exposure to hydrogen tested at ΔK=1.20 MPa[m^0.5]: *a*) indication of different zones using optical microscopy, and b) the indication of the first three striations using SEM observation.

Considering a stepwise SCG behaviour, the cyclic stress builds up ahead of the crack tip and accumulates the damage, until a point where the crack jumps forward and arrests; then, releases the accumulated stress and leaves a striation mark on the fracture surface (Figure 7a). The stepwise SCG behaviour at a micromechanics level can be attributed to the crack opening in the longitudinal direction that is obtained from the fatigue test equipment. Based on the PENT test methodology, the SCG rate can be approximately considered the same as the rate of crack opening displacement for a given condition [10]. Figure 7b illustrates an example of this correlation, showing Δ crosshead displacement (=maximum crosshead displacement-minimum crosshead displacement) values as a function of the loading cycles.

Neglecting the first jump at the beginning of the test which is due to adjusting the equipment's grips with the CPENT sample, the plot of Δ crosshead displacement versus cycles shows a plateau for almost the first 200K cycles. Then, the first step in the curve marks the point of the 1st striation occurrence, and the following steps can be related to the occurrence of the next striation and so on until a sharp jump in the curve is visible which is due to the final ductile failure. To identify the occurrence of the striations which is linked to the steps in the Δ crosshead displacement versus cycle curve, the slope of the curve (m) was calculated using the following equation:

$$m = \frac{Displacement_2 - Displacement_1}{Cycle_2 - Cycle_1} \qquad \text{Eq. 2}$$

When the damage is building up ahead of the crack tip in the craze zone, the slope of the displacement curve does not significantly change. After jumping the crack to the craze boundary and forming a visible striation mark, a significant change in the slope of the displacement curve can be observed (Figure 8b). Therefore, a point where a significant peak is observed in the slope curve can be attributed to the cycle that resulted in the formation of a striation mark. Subsequently, the time taken to reach each striation can be determined. As indicated in Figure 8b, the time to the 1st striation initiation starts from the first cycle and ends when the 1st significant change in the slope is observed. The time to the 2nd striation starts from the cycle that is linked with the 1st striation mark and ends when the 2nd striation mark is formed. The time to the other striations can be similarly measured.

As shown in Figure 8b, the ratio of the number of cycles to initiate the 1st striation to the final failure is the largest when compared with the other striations. Thus, the 1st striation plays a significant part in the total time to failure for the PE pipe. In literature, the ratio of crack initiation or 1st striation initiation to the time to final failure varies from 0.2 to 0.6 and strongly depends on the resin type [10, 25].

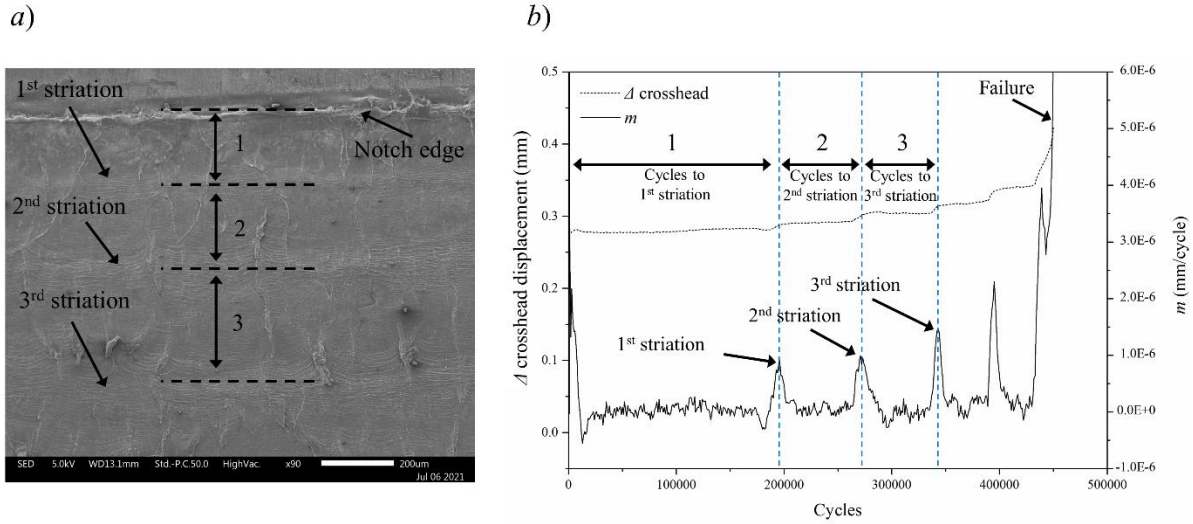

Figure 8. An approach to measuring the steady crack growth and detecting striations. *a*) indication of the first three striations on the fracture surface, and b) a comparison between the Δ crosshead vs cycle and slope vs cycle curves.

Figure 9a shows the time to failure as a function of ΔK for PE63 and PE80 at various hydrogen exposure times. For the PE80 pipe, the exposure to the hydrogen has almost no impact on the time to failure at higher ΔK values of 1.09 MPa[m^0.5] and 1.20 MPa[m^0.5] across all exposure times. However, at lower ΔKs, 0.73 MPa[m^0.5] and 0.89 MPa[m^0.5], the time to failure of the PE80 were reduced by 35% and 34%, respectively, for samples exposed to hydrogen for 90 days. For the PE63 pipe that was tested at larger ΔKs; 0.89 and 1.20, the time to failure remains almost the same when it is exposed to hydrogen for all time intervals investigated. However, at the lower ΔK of 0.65, it can be seen that the PE63 sample exposed to hydrogen gas for 90 days has a longer time to failure when compared to the PE63 non exposed sample. The time to failure of the PE63 sample that was tested at ΔK=0.65 MPa[m^0.5] is almost doubled when exposed to hydrogen for 90 days when compared to the non exposed tested at the same ΔK.

The results in Figure 9a indicate that the exposure to hydrogen does not change the time to failure of the PE63 and PE80 samples tested at larger ΔKs, which suggests that the stress has a more significant impact on the failure rather than exposure to hydrogen. On the other hand, for samples tested at lower ΔKs, the exposure to hydrogen is the governing factor in determining the time to failure.
As previously discussed, the time to the 1st striation for the non-exposed sample was a significant portion of the total time to failure. It can be seen in Figure 9b that when the samples are exposed to hydrogen, again the time to the 1st striation is the dominant portion of the total time to failure, this is true for both PE resin types and all ΔKs investigated here.

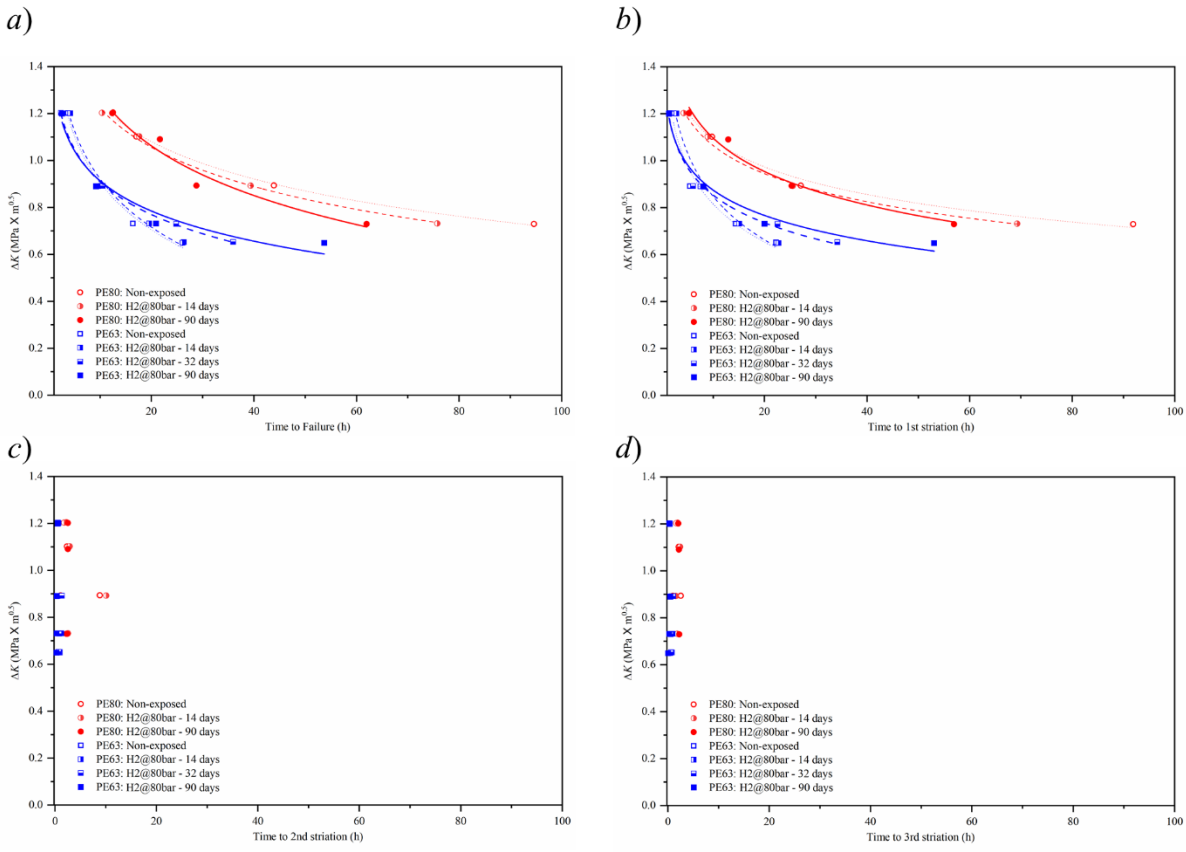

Figure 9. *a*) Time to failure, b) time to 1st striation initiation, c) time to 2nd striation initiation and d) time to 3rd striation initiation as a function of ΔK for PE63 and PE80 pipe samples that were differently exposed to hydrogen.

Since the time to failure is a combination of both the crack initiation and forming of the 1st striation, as well as the crack propagation by forming the other striations, the time needed to initiate the following two striations (2nd and 3rd striations) are also investigated in Figure -c and d. The higher-order striations can also be observed on the fracture surface, but their impact on total time to failure is significantly less. Figure 9c and d reveal that the change in the applied cyclic stress by various ΔKs had no impact on the time to initiate the 2nd and 3rd striations. After the 1st striation initiation; therefore, the progress of the crack through the sample does not appear to be significantly influenced by the applied stress beyond initiation, and hydrogen has no impact on the time to the higher-order striations.

Considering Figure 9a and b, the ratio of the time to the 1st striation initiation to the time to failure decreases by an increase in the ΔK value. This ratio varies from about 0.85 to 0.99 for the lowest ΔKs, and varies from about 0.40 to 0.68 for the highest ΔKs, depending on the particular resin and hydrogen exposure time. When decreasing the ΔK, the crack tends to be detained in rather large plastic zones for a long time before crack propagation through the 2nd and the following striations starts. For the PE63 sample which was exposed to hydrogen for 90 days and tested at ΔK=0.65, this ratio is about 0.99 and suggests that the crack was arrested in the 1st striation position for almost the total time to failure and the progress towards the following striations happened in a very short period, which suggests that hydrogen gas may have changed to some extent the crack growth and crack initiation kinetics. To explain this change in SCG kinetics X-Ray Diffraction, XRD, is used to examine the crystalline orinetation.

XRD is a non-destructive analytical technique that provides useful information about the crystallographic structure of materials. X-ray diffractometry was performed on PE63 before and after 80 bar hydrogen exposure using a Panalytical X-pert Pro MRD texture goniometer on focus mode with a Ni-filtered Cu Kα radiation source at 40 kV acceleration voltage and 30 mA current over the 2θ range from 10^{o} to 70^{o} at a rate of 0.01^{o} every 3 seconds. The x-ray diffractograms of the non-exposed (black) and exposed (dotted red) conditions are shown in Figure 9. The characteristic (110) and (200) crystal planes can be seen in both diffractograms. However, for the hydrogen exposed condition (dotted red) a decrease in intensity of the (110) plane coupled with an intensity increase of the (200) plane is observed. This likely suggest that a shift in the crystal orientation have occurred causing one crystal plane to become more 'in focus' of the incident beam while the other one is shifting away from the beam focus. This slight rotation in the crystal orientation after hydrogen exposure likely also explains the difference in crack growth described above

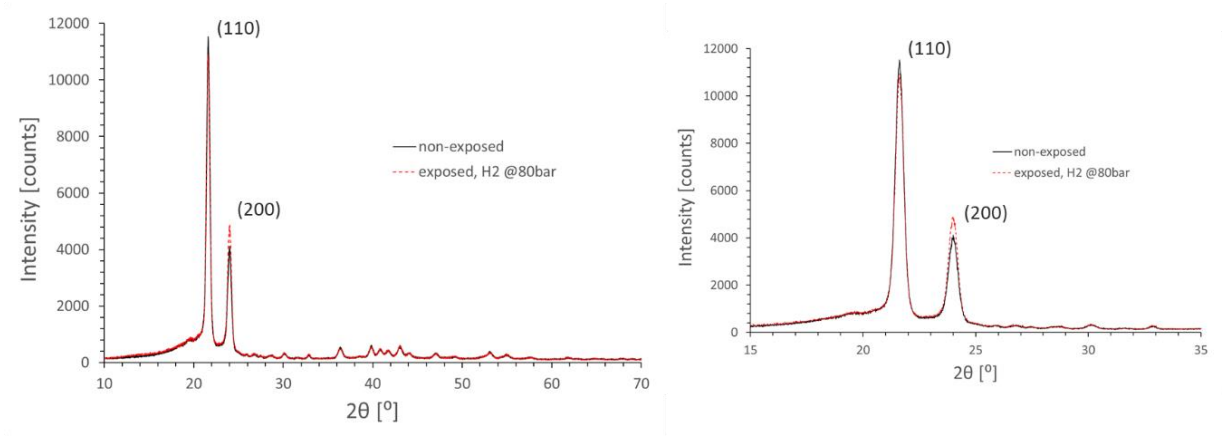

Figure 10 The x-ray diffractograms of the APA36 (PE63) sample from previous report where (black) is the non-exposed and (red) the 180 days exposed condition.

5. CONCLUSIONS

This paper outlined the reposnse of elastomers and PE pipe to hydrogen. Specifically two commercially available general use NBR70 elastomers were investigated and showed radically different responses to hydrogen. Supplier 1 NBR70 had a significantly negative response when exposed to H_2 gas showing a decrease in storage modulus and reduced recovery rate response after being compressed. In contrast NBR70 supplier 2 showed a slight increase in storage modulus and thus an improved recovery rate for the compression set measurements. HNBR, a technical elastomer used extensively in the gas industry, was included in the study and showed an increase in flexibility with H_2 gas and improved recovery rate for the compression set measurements. This study was conducted at low to moderate pressures relative to previous pressures reported and shows that even at these lower pressures changes are observed in the elastomer material properties, however the changes are not permeant. On the failure mode for PE, it was shown that the time to failure was influenced by exposure to H_2 gas and that was most obvious for PE63 at higher K_{max} values, whereby the initiation step was most impacted. To support this, XRD was conducted on the PE63 exposed sample revealing a change in the crystal orientation.

6. ACKNOWLEDGEMENTS

This work is funded by the Future Fuels CRC, supported through the Australian Government's Cooperative Research Centres Program. The cash and in-kind support from the industry, government and university participants is gratefully acknowledged.

7. REFERENCES

[1] N. Brandon and Z. Kurban, "Clean energy and the hydrogen economy," *Philosophical Transactions of the Royal Society A: Mathematical, Physical and Engineering Sciences,* vol. 375, no. 2098, p. 20160400, 2017.

[2] T. Capurso, M. Stefanizzi, M. Torresi, and S. Camporeale, "Perspective of the role of hydrogen in the 21st century energy transition," *Energy Conversion and Management,* vol. 251, p. 114898, 2022.

[3] P. G. Hartley and V. Au, "Towards a Large-Scale Hydrogen Industry for Australia," 2020.

[4] M. Noussan, P. P. Raimondi, R. Scita, and M. Hafner, "The role of green and blue hydrogen in the energy transition—a technological and geopolitical perspective," *Sustainability,* vol. 13, no. 1, p. 298, 2021.

[5] M. Ball and M. Weeda, "The hydrogen economy – Vision or reality?11This paper is also published as Chapter 11 'The hydrogen economy – vision or reality?' in Compendium of Hydrogen Energy Volume 4: Hydrogen Use, Safety and the Hydrogen Economy, Edited by Michael Ball, Angelo Basile and T. Nejat Veziroglu, published by Elsevier in 2015, ISBN: 978-1-78242-364-5. For further details see: http://www.elsevier.com/books/compendium-of-hydrogen-energy/ball/978-1-78242-364-5," *International Journal of Hydrogen Energy,* vol. 40, no. 25, pp. 7903-7919, 2015/07/06/ 2015, doi: https://doi.org/10.1016/j.ijhydene.2015.04.032.

[6] N. Aibada, M. Ramachandran, K. K. Gupta, and P. Raichurkar, "Review on various gaskets based on the materials, their characteristics and applications," *International Journal on Textile Engineering and Processes,* vol. 3, no. 1, pp. 13-18, 2017.

[7] H. Fujiwara, "Analysis of Acrylonitrile Butadiene Rubber (NBR) Expanded with Penetrated Hydrogen due to High Pressure Hydrogen Exposure," *International Polymer Science and Technology,* vol. 44, pp. 41-48, 03/01 2017, doi: 10.1177/0307174X1704400308.

[8] S. Nishimura, "Fracture Behaviour of Ethylene Propylene Rubber for Hydrogen Gas Sealing under High Pressure Hydrogen," *International Polymer Science and Technology,* vol. 41, pp. 27-34, 06/01 2014, doi: 10.1177/0307174X1404100606.

[9] L. Zhu, C. S. Cheung, W. Zhang, and Z. Huang, "Compatibility of different biodiesel composition with acrylonitrile butadiene rubber (NBR)," *Fuel,* vol. 158, pp. 288-292, 2015.

[10] H. a. Ismail and H. Ahmad, "The properties of acrylonitrile-butadiene rubber (NBR) composite with halloysite nanotubes (HNTs) and silica or carbon black," *Polymer-Plastics Technology and Engineering,* vol. 52, no. 12, pp. 1175-1182, 2013.
[11] K. Hu, D. D. Kulkarni, I. Choi, and V. V. Tsukruk, "Graphene-polymer nanocomposites for structural and functional applications," *Progress in Polymer Science,* vol. 39, no. 11, pp. 1934-1972, 2014/11/01/ 2014, doi: https://doi.org/10.1016/j.progpolymsci.2014.03.001.
[12] W. Balasooriya, C. Clute, B. Schrittesser, and G. Pinter, "A Review on Applicability, Limitations, and Improvements of Polymeric Materials in High-Pressure Hydrogen Gas Atmospheres," *Polymer Reviews,* pp. 1-36, 2021, doi: 10.1080/15583724.2021.1897997.
[13] Y. Zheng *et al.*, "A review on effect of hydrogen on rubber seals used in the high-pressure hydrogen infrastructure," *International Journal of Hydrogen Energy,* vol. 45, no. 43, pp. 23721-23738, 2020/09/03/ 2020, doi: https://doi.org/10.1016/j.ijhydene.2020.06.069.
[14] J. Yamabe, S. Nishimura, and A. Koga, "A Study on Sealing Behavior of Rubber O-Ring in High Pressure Hydrogen Gas," *SAE International Journal of Materials and Manufacturing,* vol. 2, pp. 452-460, 10/15 2009, doi: 10.4271/2009-01-0999.
[15] H. Fujiwara, H. Ono, and S. Nishimura, "Degradation behavior of acrylonitrile butadiene rubber after cyclic high-pressure hydrogen exposure," *International Journal of Hydrogen Energy,* vol. 40, no. 4, pp. 2025-2034, 2015/01/30/ 2015, doi: https://doi.org/10.1016/j.ijhydene.2014.11.106.
[16] De Silva, R., T. Hilditch, and N. Byrne, *Assessing the integrity of in service polyethylene pipes.* Polymer Testing, 2018(67): p. 228-233.
[17] Liu, Y., et al., *A Time Dependent Process Zone Model for Slow Crack Growth of Polyethylene Pipe Material. .* Journal of Physics: Conference Series, 2020(1634(1)): p. 012140.
[18] Qian, Y.-f., et al., *Experimental Study on the Fatigue Crack Growth and Overload Effect in Medium Density Polyethylene.* Journal of Materials Engineering and Performance, 2020(29(10)): p. 6681-6690.
[19] Frank, A., et al., *Fracture Mechanics Lifetime Prediction of Polyethylene Pipes. .* Journal of Pipeline Systems Engineering and Practice, 2019. 10(1): p. 04018030.
[20] Liu, Y., et al., *A Time Dependent Process Zone Model for Slow Crack Growth of Polyethylene Pipe Material.* Journal of Physics: Conference Series, 2020. 1634(1): p. 012140.
[21] Qian, Y.-f., et al., *Experimental Study on the Fatigue Crack Growth and Overload Effect in Medium Density Polyethylene.* Journal of Materials Engineering and Performance, 2020. 29(10): p. 6681-6690.
[22] Nguyen, K.Q., et al., *Long-term testing methods for HDPE pipe - advantages and disadvantages: A review.* Engineering Fracture Mechanics, 2021. 246: p. 107629.
[23] Frank, A., et al., *Fracture Mechanics Lifetime Prediction of Polyethylene Pipes.* Journal of Pipeline Systems Engineering and Practice, 2019. 10(1): p. 04018030.
[24] Nezbedová, E., et al., *The applicability of the Pennsylvania Notch Test for a new generation of PE pipe grades.* Polymer Testing, 2013. 32(1): p. 106-114.
[25] Pinter, G., W. Balika, and R.W. Lang, *A correlation of creep and fatigue crack growth in high density poly(ethylene) at various temperatures*, in *European Structural Integrity Society*, L. Rémy and J. Petit, Editors. 2002, Elsevier. p. 267-275.
[26] Frank, A., et al., *Comparison of accelerated tests for PE grades lifetime assessment.* Proceedings of Plastic Pipes, 2012. 16(24): p. 26.09.
[27] Krishnaswamy, R.K., A.M. Sukhadia, and M.J. Lamborn, *Is PENT a True Indicator of PE Pipe Slow Crack Growth Resistance?* Bulletin, Performance Pipe, Plano, TX, Report No. PP818-TN. http://www. hdpe. ca/wp-content/uploads/2016/03/PP818-TN-PENT-Slow-Crack-Growth-Resistance. pdf, 2007.
[28] Brown, N. and J.M. Crate, *Analysis of a Failure in a Polyethylene Gas Pipe Caused by Squeeze off Resulting in an Explosion.* Journal of Failure Analysis and Prevention, 2012. 12(1): p. 30-36.
[29] *ISO 18489: Polyethylene (PE) materials for piping systems — Determination of resistance to slow crack growth under cyclic loading — Cracked Round Bar test method*. 2015, International Organization for Standardization.